Hindawi
Geofluids
Volume 2021, Article ID 6668799, 8 pages
https://doi.org/10.1155/2021/6668799

Research Article

Determining Triaxial Stress Sensitivity of Oil Reservoir Rocks without Fluid Flooding

Zhihang Li[1] and Xiong Hu[2]

[1]*Department of Civil Engineering, Monash University, 3800, Australia*
[2]*China United Coalbed Methane National Engineering Research Center Co., Ltd., Beijing 100095, China*

Correspondence should be addressed to Xiong Hu; huxiongcnpc@163.com

Received 8 December 2020; Revised 6 March 2021; Accepted 25 March 2021; Published 15 April 2021

Academic Editor: Qingquan Liu

The sensitivity of oil reservoir rocks to stress is the basis for oilfield development, which determines the production method employed in the field. Therefore, it is critical to understand the stress sensitivity behavior of oil reservoir rocks in an oilfield. In this paper, a novel method for determining the stress sensitivity of oil reservoir rocks by triaxial stress testing without fluid flooding was proposed. It measures the triaxial stress and strain of the core rock samples, and based on which, the core porosity and permeability under stress can be evaluated by theoretical model. In the model, the pores of the core were assumed to be a bundle of capillaries and the necessary relationship was derived to calculate the changes of porosity and permeability of the core samples caused by the strain. Through comparison with and analysis of experimental results obtained for various rock core samples under different stress and strain conditions, it is observed that the theoretical model match well with that of the experiments. This method provides a new approach for the stress sensitivity analysis of oil reservoirs without fluid flooding.

1. Introduction

The variation of oil reservoir core porosity and permeability under stress is called the reservoir rock stress sensitivity, which is the basis for reservoir production mode selection. If an oil reservoir rock is relatively stress sensitive, it is necessary to take immediate actions to avoid porosity and permeability reduction. The production potential of gas hydrates mainly depends on permeability characteristics of the bearing sediments as high permeability could promote the production rate [1]. And the enhancement of gas effective permeability with increased gas saturation weakens with higher complexity and lower discreteness of a pore network. A less complex and more discrete pore network better benefits the gas injectivity index [2].

Therefore, in the late 1980s, scientists began to carry out research on the stress sensitivity of oil reservoirs, mainly by core flooding experiments [3, 4]. In the experiments, a certain confining pressure is applied to a core sample in three directions [5, 6]; then, crude oil or nitrogen gas is driven to flow through the core sample, and the pressure and flow rate at both ends of the core are [7–11]. The permeability of the core sample is calculated based on the Darcy equation, through which the permeability of the core samples under different stress and strain can be obtained by varying the confining pressure. Then, the characteristics of stress sensitivity of the rock core are obtained by analyzing the empirical law of permeability under different confining pressures [12]. It is the conventional method of obtaining reservoir rock stress sensitivity which has been widely used by oilfield scientists [13–15].

However, such method faces a few problems which still need to be tackled with urgently: First, it is difficult to apply stress simultaneously in three different directions (x, y, and z) during the actual production stage. In realistic producing oilfield, the stress on rocks is always applied from the top, which is different from the laboratory situation where the stress is from three directions [16–18]. Second, the method involves measuring the pressure and flow rate of the flooding liquid or gas at both ends of the rock core, while the permeability is calculated by the Darcy formula. If the sealing between the core sample and the core holder becomes

defective during the experiment, the fluid would leak rather than fully pass through the core sample. The fluid may flow through the gap between the core sample and the core holder instead, and the measured flow rate will be different from that of the real situation. Thus, the evaluated permeability may be deviated from the actual value of the reservoir core sample [19, 20].

The changes of porosity and permeability of artificial tight core with stress were studied by Cao and Lei [21] who performed lithologic flow experiment. And the stress sensitivity of the process of pressurization and unloading of tight reservoir is analyzed through the laboratory experiment of stress sensitivity hysteresis of core. The research shows that in the early stage of compression, under the joint action of rock structure deformation and bulk deformation, core permeability decreases rapidly with the increase of effective stress. When the effective stress exceeds a certain value, rock structure deformation tends to be stable, only bulk deformation occurs, and core permeability changes tend to be flat. In the unloading stage, the deformation of the rock body is gradually restored with the reduction of effective stress, while the structural deformation cannot be restored, core permeability cannot be completely restored, and stress sensitivity hysteresis phenomenon is obvious.

Chen et al. [22] mainly study the stress-strain characteristics and permeability variation of rock under confining pressure unloading condition and obtain the understanding of the by-correlation between permeability and volume strain during loading and unloading process.

Yaser et al. [23] studied the pore structure, porosity, and permeability of carbonate rocks under pressure with the combination of experiments and microscopic images. The results showed that the porosity and permeability of calcalite samples decreased with the increase of pressure load.

Liu et al. [24] conduct an experimental study of salt rock deformation and strength under different confining pressures using the salt rocks from Pingdingshan, China. The results show that the pure salt rock shows great brittleness and failure in uniaxial test. However, the presence of impurities improved the strength of the sample, and the strength of rock salt showed strong alkaline strain hardening with the increase of impurity content. Experiment shows that the higher the confining pressure, the more obviously lag expands occur.

Sui et al. [25] research the deformation of the core by using the digital core method, and the simulated pores in the digital core are simplified into three abstract types: long ellipsoid, flat ellipsoid, and ellipsoid. Based on the theory of microscopic mechanics, the three-dimensional spherical pore model of digital core is established. The constitutive relation of pore microstructure deformation of different types is studied by using Eshelby equivalent medium theory, and the influence of pore structure on pore volume compressibility under the condition of single pore and porous elastic deformation is studied. The results show that the numerical core of pore volume compression coefficient is closely related to the porosity, pore aspect ratio, and volume ratio of different types of pores. The compressibility of the long ellipsoid hole coefficient is positively correlated with the hole width ratio, while the compressibility of the flat ellipsoid hole coefficient is negatively correlated with the hole width ratio. When the mean value of hole width ratio satisfying Gaussian distribution is the same, the larger the hole width ratio is, the larger the pore aspect ratio range is, the higher the compression coefficient of long ellipsoid and flat ellipsoid hole is, and the greater the deformation is under the same stress condition. Table 1 summarizes the existing experiments.

In order to avoid the problems discussed above, in this paper, a new testing method without fluids involved during the process was proposed. The method is to test the triaxial stress and strain of rock core samples, which eliminates the challenge of sealing between the annulus core and its holder and prevents fluids from leaking out therefrom. And to make the testing happen, a novel mathematical model is established to calculate the porosity and permeability of the oil reservoir rocks based on applied stress and strain data. Actual applications demonstrate that the method is an effective approach for stress sensitivity analysis of rocks and is simpler and more advantageous than the conventional methods.

2. Mathematical Model for Simulating Porosity and Permeability Changes under Stress

Here, The mathematical model is established for calculating the oil reservoir rock porosity and permeability from the experimentally measured triaxial stress and strain data. And how to process and incorporate the experimental data into the model is a critical factor.

2.1. Model for the Relationship between Volumetric Strain and Stress. During the production stage of an oil reservoir, the formation fluid pressure decreases. This disturbs the static equilibrium of the formation and causes rock deformation under stress, which creates volumetric strain to the core rock, as illustrated in Figure 1.

Assuming that the stresses in the x, y, and z triaxial directions are $\sigma_x, \sigma_y, \sigma_z$, then they can be analyzed in two situations: one is the elastic deformation, and the other is the elastoplastic deformation.

2.1.1. Analysis for Elastic Deformation. According to the laws of elastic mechanics, the relationship between volumetric strain and stress can be obtained by the general Hooke's law. For the x, y, and z directions, the volumetric strain can be expressed as

$$\begin{cases} \varepsilon_x = \dfrac{1}{E}\left[\sigma_x - \mu\left(\sigma_y + \sigma_z\right)\right], \\ \varepsilon_y = \dfrac{1}{E}\left[\sigma_y - \mu\left(\sigma_x + \sigma_z\right)\right], \\ \varepsilon_z = \dfrac{1}{E}\left[\sigma_z - \mu\left(\sigma_x + \sigma_y\right)\right], \end{cases} \tag{1}$$

where E is Young's Modulus and μ is Poisson's ratio, and the volumetric strain ε_v is expressed as

$$\varepsilon_v = \varepsilon_x + \varepsilon_y + \varepsilon_z. \tag{2}$$

Table 1: Existing experiment.

Experiment	References
Porosity and permeability	Cao and Lei [21]
Stress-strain characteristics	Chen et al. [22]
Pore structure, porosity, and permeability	Yaser et al. [23]
Rock deformation and strength	Liu et al. [24]
Simulated deformation of the core with digital method	Sui et al. [25]

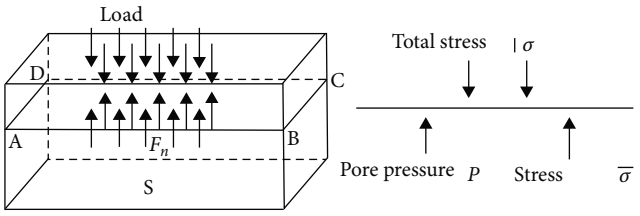

Figure 1: Simulation of rock stress and strain changes.

Combining equations (1) and (2) gives

$$\varepsilon_v = \frac{1-2\mu}{E}\left(\sigma_x + \sigma_y + \sigma_z\right). \tag{3}$$

2.1.2. Analysis for Elastoplastic Deformation. Under the experiment condition, Young's Modulus (E) of rocks is not constant for elastoplastic deformation, which increases with the stress. The experiments results showthat satisfies the following empirical law:

$$E = \frac{d\sigma}{d\varepsilon} = b(\sigma)^q, \tag{4}$$

where b and q represent the nonlinear elastic deformation index, if b and q are equal to 1, which represent elastic deformation.

According to the theory of elastic mechanics,

$$d\varepsilon_x = \frac{d\sigma_x}{E_x} - \mu\frac{d\sigma_y}{E_y} - \mu\frac{d\sigma_z}{E_z}. \tag{5}$$

From equation (4),

$$E_y = b\left(\sigma_y\right)^q, \tag{6}$$

$$E_z = b(\sigma_z)^q. \tag{7}$$

Substituting equations (6) and (7) into equation (5) gives

$$d\varepsilon_x = \frac{1}{b}\left[{\sigma_x}^{-q}d\sigma_x - \mu{\sigma_y}^{-q}d\sigma_y - \mu{\sigma_z}^{-q}d\sigma_z\right]. \tag{8}$$

Integrating the both sides of equation (8) gives

$$\varepsilon_x = \frac{1}{b}\frac{1}{1-q}\left[\sigma_x^{1-q} - \mu\left(\sigma_y^{1-q} + \sigma_z^{1-q}\right)\right]. \tag{9}$$

Similarly, for y and z directions, it gives

$$\cdots\varepsilon_y = \frac{1}{b}\frac{1}{1-q}\left[\sigma_y^{1-q} - \mu\left(\sigma_x^{1-q} + \sigma_z^{1-q}\right)\right], \tag{10}$$

$$\cdots\varepsilon_z = \frac{1}{b}\frac{1}{1-q}\left[\sigma_z^{1-q} - \mu\left(\sigma_x^{1-q} + \sigma_y^{1-q}\right)\right]. \tag{11}$$

From equations (2), (9), (10), and (11), the relationship between volumetric strain and stress is obtained as

$$\cdots\varepsilon_v = \frac{1-2\mu}{b(1-q)}\left[\sigma_x^{1-q} + \sigma_y^{1-q} + \sigma_z^{1-q}\right]. \tag{12}$$

When q is equal to 0 in equation (12), it becomes a simplified expression of equation (3), which is an expression of an elastic medium. Therefore, equation (12) is universally applicable regardless of elastic or elastoplastic deformation.

2.2. Model for the Relationship between Porosity and Volumetric Strain. The oil reservoir rock is composed of framework and pore space. It is assumed that when the oil reservoir rock is subjected to effective stress, the core framework is not deformed, and only the pore space will be compressed, resulting in volumetric strain, as shown in Figure 2.

According to the definition of porosity,

$$\phi = \frac{V_b - V_r}{V_b} = 1 - \frac{V_r}{V_b}, \tag{13}$$

where V_b is the total volume of the rock sample and V_r is the pore volume of the rock sample.

When external stress acts on the porous core, the porosity changes from the initial state of ϕ_0 to the current state of ϕ, with a volumetric strain of ε_v generated. The following equation indicates the relationship.

$$\Delta V_b = V_b\varepsilon_v. \tag{14}$$

At constant temperature, equation (14) can be substituted into equation (13), which gives an expression for the porosity after the core volume change is obtained.

$$\phi = 1 - \frac{V_r}{Vb + \Delta V_b}. \tag{15}$$

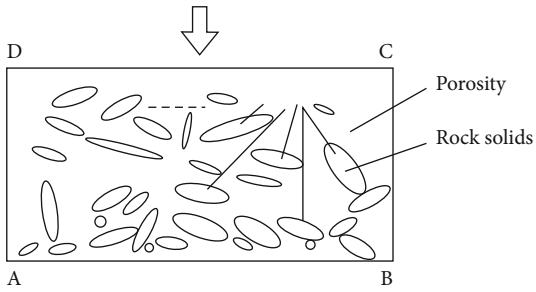

Figure 2: Rock porosity changes under compression and strain.

Figure 3: The triaxial stress core rock experimental instrument.

And substituting equations (13) and (14) into equation (15) gives

$$\phi = 1 - \frac{1 - \phi_0}{1 + \varepsilon_v}. \tag{16}$$

Then, the change in porosity at different volumetric strains can be calculated by equation (16).

2.3. Model for Relationship between Rock Permeability and Volumetric Strain. The permeability of a rock is closely related to its strain. Here, the complex porous medium is simplified into a series of equal diameter capillary tubes [3]. The relationship between the theoretical rock permeability and rock porosity can be obtained according to the Kozeny-Carman equation.

$$k = \frac{\phi}{k_z S_p{}^2}, \tag{17}$$

where k_z is a constant of approximately 5, ϕ the porosity, and S_p/cm^2 the pore surface area of volume of the pore medium. Equation (17) indicates that change in porosity is the main factor causing changes in the permeability of the rock sample.

Substituting equation (16) into (17), the mathematical model for the changes in rock permeability with volumetric strain is derived as

$$\frac{k}{k_0} = \frac{1}{(1 + \varepsilon_v)^2} \left(1 + \frac{\varepsilon_v}{\phi_0}\right)^2. \tag{18}$$

From equation (18), the permeability of the rock core can be calculated once the volumetric strain and the initial porosity of the rock core are known.

3. Application on Rock Stress Sensitivity Analysis with Triaxial Stress Experiments

3.1. Sample Preparation. The rock core sample used in the verification experiment is from the Tahe Oilfield in Xinjiang Province in China. The carbonate oil reservoir is located at a depth of about 3,500 meters. A standard core rock sample was prepared for triaxial stress sensitivity experiment. The experimental setup is shown in Figure 3.

In order to simplify the evaluation of stress, it was assumed that the confining and the axial pressures are equal. The experiment was done in the applied pressure range from 2 MPa to 65 MPa, and the process of loading stress was in three steps, as illustrated as follows:

Step 1: firstly, a low confining pressure of 2 MPa was loaded onto the side of the sample; then, the same amount of axial pressure was applied. The radial and axial strains under the confining and axial pressures are measured;

Step 2: secondly, the confining pressure and its corresponding axial pressure were increased to 65 MPa, and the axial and radial strains were measured under this condition;

Step 3: finally, keeping the pressure on the rock until the rock sample was crushed. The confining and axial pressures were loaded from 2 MPa to 65 MPa.

3.2. Analysis and Application of Experimental Results. The radial and axial strain data of the rock samples under different stresses were obtained by experiments, and the corresponding volumetric strain data under the conditions were calculated by equation (12). The results are shown in Table 2.

The data in Table 2 are used to evaluate the corresponding changes in porosity and permeability according to equations (16) and (18), respectively. Meanwhile, the porosity and permeability damage rate was evaluated as well, and the results are shown in Table 3.

As shown in Figure 4, the volume strain of the core has a good power relationship with the effective stress.

Figure 5 shows that for the carbonate rock, the porosity, and effective stress satisfy the relationship of $\phi = 0.0415 e^{-0.003p}$. The porosity decreases with increase in the effective stress. Meanwhile, the porosity decreased more rapidly in the initial stage when the effective stress was less than 20 MPa.

From Figure 6 it is realized that porosity and effective stress of the core sample satisfy the relationship of $k = 0.022e^{-0.0059p}$. The permeability decreased with increase in the effective stress. Meanwhile, the reduction rate of the permeability increased when the effective stress is less than 20 MPa.

Figure 7 shows that the dimensionless porosity and effective stress of the core sample satisfy the power relationship of $\phi/\phi_0 = 0.9773e^{-0.003p}$.

Table 2: Data of deformation and volumetric strain under different axial stress.

Confining stress (MPa)	Axial stress (MPa)	Radial deformation	Axial deformation	Radial strain	Axial strain	Volumetric strain
2	2	-5.8080*E*-03	1.5236*E*-02	-2.2866*E*-04	3.7995*E*-04	8.3705*E*-04
4	4	-9.0040*E*-03	2.3964*E*-02	-3.5449*E*-04	5.9761*E*-04	1.3060*E*-03
6	6	-1.1410*E*-02	3.1008*E*-02	-4.4921*E*-04	7.7327*E*-04	1.6708*E*-03
8	8	-1.3538*E*-02	3.7248*E*-02	-5.3299*E*-04	9.2888*E*-04	1.9936*E*-03
10	10	-1.5528*E*-02	4.3108*E*-02	-6.1134*E*-04	1.0750*E*-03	2.2960*E*-03
13	13	-1.8232*E*-02	5.1420*E*-02	-7.1780*E*-04	1.2823*E*-03	2.7155*E*-03
16	16	-2.0722*E*-02	5.9676*E*-02	-8.1583*E*-04	1.4882*E*-03	3.1167*E*-03
19	19	-2.2960*E*-02	6.8996*E*-02	-9.0394*E*-04	1.7206*E*-03	3.5245*E*-03
22	22	-2.5042*E*-02	7.7160*E*-02	-9.8591*E*-04	1.9242*E*-03	3.8912*E*-03
25	25	-2.7950*E*-02	6.5032*E*-02	-1.1004*E*-03	1.6217*E*-03	3.8178*E*-03
30	30	-2.8386*E*-02	1.1482*E*-01	-1.1176*E*-03	2.8634*E*-03	5.0909*E*-03
35	35	-3.0738*E*-02	1.2770*E*-01	-1.2102*E*-03	3.1844*E*-03	5.5956*E*-03
40	40	-3.2838*E*-02	1.4039*E*-01	-1.2928*E*-03	3.5009*E*-03	6.0759*E*-03
45	45	-3.4714*E*-02	1.5415*E*-01	-1.3667*E*-03	3.8441*E*-03	6.5651*E*-03
50	50	-3.6462*E*-02	1.6672*E*-01	-1.4355*E*-03	4.1576*E*-03	7.0146*E*-03
55	55	-3.8830*E*-02	1.7214*E*-01	-1.5287*E*-03	4.2927*E*-03	7.3347*E*-03
60	60	-3.9602*E*-02	1.8980*E*-01	-1.5591*E*-03	4.7332*E*-03	7.8343*E*-03
65	65	-4.1014*E*-02	2.0234*E*-01	-0.001614724	0.005045985	0.008256544

Table 3: Data of porosity and permeability damage rate under different confining stress.

Confining stress (MPa)	Axial stress (MPa)	Dimensionless porosity	Dimensionless permeability	Absolute value of permeability reduction (mD)	Absolute value porosity reduction	Porosity damage rate	Permeability damage rate
2	2	0.9811	0.9627	8.59*E*-04	8.02*E*-04	1.89%	3.73%
4	4	0.9705	0.9421	1.33*E*-03	1.25*E*-03	2.95%	5.79%
6	6	0.9623	0.9261	1.70*E*-03	1.60*E*-03	3.77%	7.39%
8	8	0.9550	0.9121	2.02*E*-03	1.91*E*-03	4.50%	8.79%
10	10	0.9482	0.8991	2.32*E*-03	2.20*E*-03	5.18%	10.09%
13	13	0.9387	0.8812	2.74*E*-03	2.61*E*-03	6.13%	11.88%
16	16	0.9296	0.8642	3.13*E*-03	2.99*E*-03	7.04%	13.58%
19	19	0.9203	0.8471	3.52*E*-03	3.39*E*-03	7.97%	15.29%
22	22	0.9120	0.8318	3.87*E*-03	3.74*E*-03	8.80%	16.82%
25	25	0.9137	0.8349	3.80*E*-03	3.67*E*-03	8.63%	16.51%
30	30	0.8847	0.7828	5.00*E*-03	4.90*E*-03	11.53%	21.72%
35	35	0.8732	0.7626	5.47*E*-03	5.39*E*-03	12.68%	23.74%
40	40	0.8623	0.7436	5.91*E*-03	5.85*E*-03	13.77%	25.64%
45	45	0.8511	0.7245	6.35*E*-03	6.33*E*-03	14.89%	27.55%
50	50	0.8408	0.7071	6.75*E*-03	6.76*E*-03	15.92%	29.29%
55	55	0.8335	0.6949	7.03*E*-03	7.07*E*-03	16.65%	30.51%
60	60	0.8221	0.6759	7.47*E*-03	7.56*E*-03	17.79%	32.41%
65	65	0.8124	0.6601	7.83*E*-03	7.97*E*-03	18.76%	33.99%

As shown in Figure 8, the dimensionless permeability and effective stress of the core sample satisfy the exponential relationship of $k/k_0 = 0.9552e^{-0.0069p}$.

The results show that the oil reservoir core porosity and permeability under stress can be well evaluated using the mathematical model together with experimental stress and strain data with no need of introducing flooding fluid.

4. Discussion

The method proposed by the paper addresses the problem of sealing and leakage of core holders in the conventional stress and flowing fluid method which provides a new approach for the stress sensitivity analysis of oil reservoirs without fluid flooding. The results of the experimental prove that the

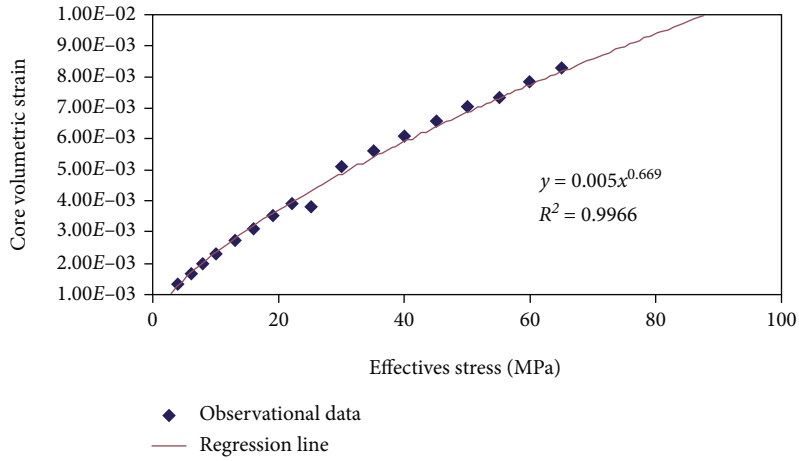

Figure 4: Relationship between core volumetric strain and effective stress.

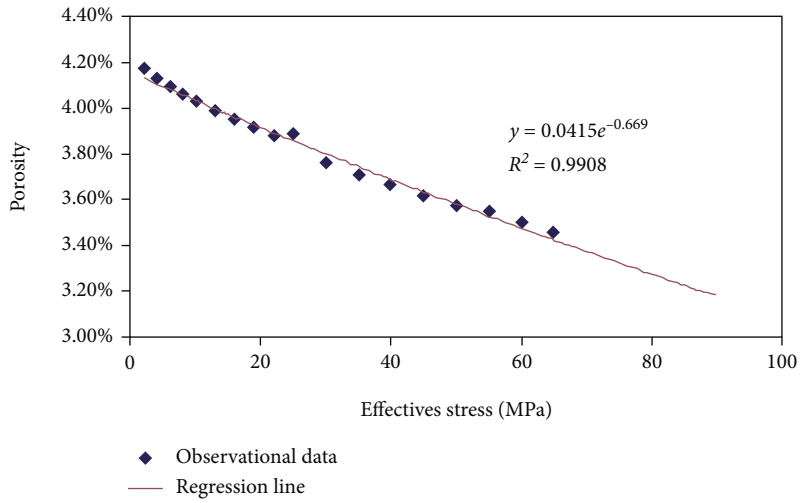

Figure 5: Relationship between porosity and effective stress.

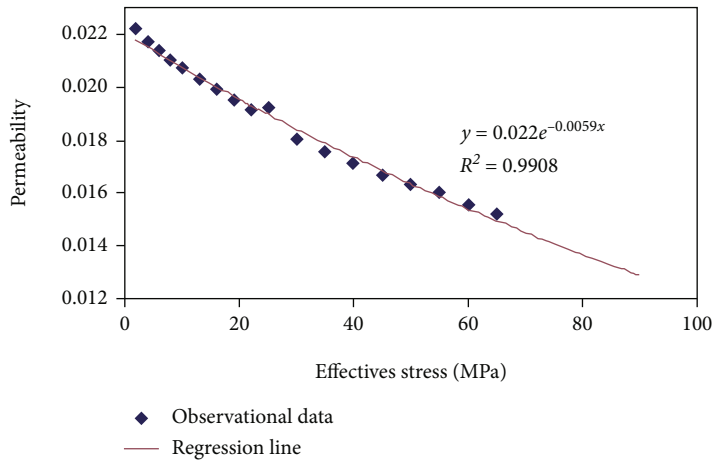

Figure 6: Relationship between permeability and effective stress.

proposed method is feasible and effective. Compared with the conventional method, the proposed method measures the triaxial stress and strain of the core rock samples and based on which, the core porosity and permeability under stress can be evaluated by theoretical model. However, the enhancement of gas effective permeability with increased gas saturation

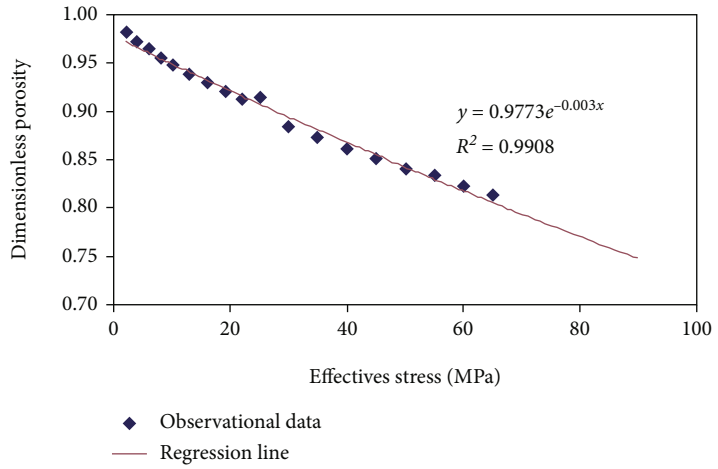

Figure 7: Relationship between dimensionless porosity and effective stress.

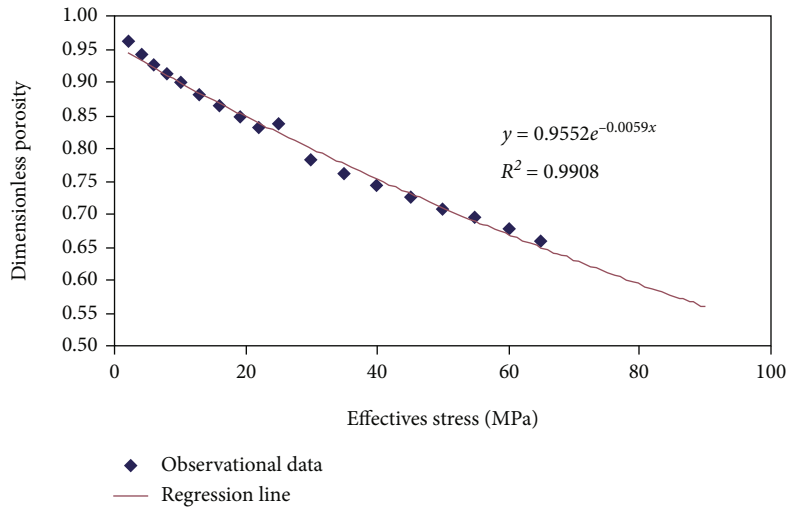

Figure 8: Relationship between dimensionless permeability and effective stress.

weakens with higher complexity and lower discreteness of a pore network. Therefore, for the rock with higher porosity, this method is less effective and the results would have deviation errors. The future work is to continuously improve the model by adding other influence factors, to achieve higher accuracy of soft rocks or rocks with microcracks.

5. Conclusion

The experimental results showed that the triaxial stress method proposed by this investigation with applying rock mechanics method to test the stress sensitivity of reservoir rocks is feasible. The experimental method is practical and simple test while the mathematical model results are reliable. It is feasible to evaluate the mathematical model for changes in permeability and porosity with stress from experimental data of triaxial stress. The calculated results matched well with the experimental results. Comparing with the conventional method of applying stress and flowing fluid through rocks by a core flooding equipment, the proposed method by this investigation avoids the problems of sealing and leakage of core holders and has other advantages as well. However, the new method is less adaptable for soft rocks or rocks with microcracks, where the results obtained would be biased.

Data Availability

The data used to support the findings of the study are included within the article.

Conflicts of Interest

The authors declared that there is no financial and personal relationships with other people or organizations that can inappropriately influence our work, and there is no professional or other personal interest of any nature or kind in any product, service, and/or company that could be construed as influencing the position presented in or the review

of the manuscript entitled, "Determining triaxial stress sensitivity of oil reservoir rocks without fluid flooding."

References

[1] G. Lei, Q. Liao, Q. Lin, L. Zhang, L. Xue, and W. Chen, "Stress dependent gas-water relative permeability in gas hydrates: a theoretical model," *Advances in Geo-Energy Research*, vol. 4, no. 3, pp. 326–338, 2020.

[2] J. Xu, Z. Chen, and R. Li, "Impacts of pore size distribution on gas injection in intraformational water zones in oil sands reservoirs," *Oil & Gas Science and Technology*, vol. 75, p. 75, 2020.

[3] F. O. Jones, "A laboratory study of the effects of confining pressure on fracture flow and storage capacity in carbonate rocks," *Journal of Petroleum Technology*, vol. 27, no. 1, pp. 21–27, 1975.

[4] C. R. Mckee, A. C. Bumb, and R. A. Koenig, "Stress-dependent permeability and porosity of coal and other geologic formations," *SPE Formation Evaluation*, vol. 3, no. 1, pp. 81–91, 1988.

[5] A. T. Gorbrov, *Abnormal Field Development*, Petroleum industry Press, Beijing, 1987.

[6] J. Geertsma, "The effect of fluid pressure decline on volumetric changes of porous rocks," *Transactions of the AIME*, vol. 210, no. 1, pp. 331–340, 1957.

[7] A. Finol and S. M. F. Ali, "Numerical simulation of oil production with simultaneous ground subsidence," *Society of Petroleum Engineers Journal*, vol. 15, no. 5, pp. 411–424, 1975.

[8] H. H. Vaziri, "Coupled fluid flow and stress analysis of oil sands subject to heating," *Journal of Canadian Petroleum Technology*, vol. 27, no. 5, 1988.

[9] J. Noorishad, M. S. Ayatollahi, and P. A. Witherspoon, "A finite-element method for coupled stress and fluid flow analysis in fractured rock masses," *International Journal of Rock Mechanics and Mining Sciences & Geomechanics Abstracts*, vol. 19, no. 4, pp. 185–193, 1982.

[10] A. Settari, P. R. Kry, and C. T. Yee, "Coupling of fluid flow and soil behaviour to model injection into uncemented oil sands," *Journal of Canadian Petroleum Technology*, vol. 28, no. 1, pp. 81–92, 1989.

[11] L. S.-K. Fung, A. D. Hiebert, and L. X. Nghiem, "Reservoir simulation with a control-volume finite-element method," *SPE Reservoir Engineering*, vol. 7, no. 3, pp. 349–357, 1992.

[12] D. T. Snow, "Anisotropic permeability of fractured Media," *Water Resources Research*, vol. 5, no. 6, pp. 1273–1289, 1969.

[13] L. S. K. Fung, "Coupled geomechanical-thermal simulation for deforming heavy oil reservoirs," *Journal of Canadian Petroleum Technology*, vol. 4, pp. 22–28, 1994.

[14] W. S. Tortike and S. M. F. Ali, "Prediction of oil sand failure due to steam-induced stresses," *Journal of Canadian Petroleum Technology*, vol. 30, no. 1, 1991.

[15] N. Cao and G. Lei, "Stress sensitivity of tight reservoirs during pressure loading and unloading process," *Petroleum Exploration and Development*, vol. 46, no. 1, pp. 138–144, 2019.

[16] G. W. Richard, "A constitutive model for the effective stress-strain behavior of oil sands," *Journal of Canadian Petroleum Technology*, vol. 10, pp. 28–38, 1993.

[17] R. C. K. Wong, A. M. Samieh, and R. L. Kuhlemeyer, "Oil sand strength parameters at low effective stress: its effects on sand production," *Journal of Canadian Petroleum Technology*, vol. 33, no. 5, pp. 44–49, 1994.

[18] W. F. Brace, J. B. Walsh, and W. T. Frangos, "Permeability of granite under high pressure," *Journal of Geophysical Research*, vol. 73, no. 6, pp. 2225–2236, 1968.

[19] S. Peng, Z. Meng, H. Wang, C. Ma, and J. Pan, "Pore and permeability test of sandstone under different confining pressures research," *Journal of Rock Mechanics and Engineering*, vol. 22, no. 5, pp. 742–746, 2003.

[20] O. Kwon, A. K. Kronenberg, A. F. Gangi, and B. Johnson, "Permeability of Wilcox shale and its effective pressure law," *Journal of Geophysical Research: Solid Earth*, vol. 106, no. B9, pp. 19339–19353, 2001.

[21] N. Cao and G. Lei, "Stress sensitivity of pressure relief process in tight reservoir," *Petroleum Exploration and Development*, vol. 46, no. 1, pp. 132–138, 2019.

[22] X. Chen, C. Tang, J. Yu, J. F. Zhou, and Y. Y. Cai, "Experimental investigation on deformation characteristics and permeability evolution of rock under confining pressure unloading conditions," *Journal of Central South University*, vol. 25, no. 8, pp. 1987–2001, 2018.

[23] S. Yaser, M. Ali, K. Ezatallah, P. Peyman, and M. Abbas, "Petrophysical property change and structural deformation experiment of carbonate reservoir," *Petroleum Exploration and Development*, vol. 46, no. 3, pp. 542–551, 2019.

[24] W. Liu, X. Zhang, H. Li, and J. Chen, "Investigation on the deformation and strength characteristics of rock salt under different confining pressures," *Geotechnical and Geological Engineering*, vol. 38, no. 6, pp. 5703–5717, 2020.

[25] W. Sui, Z. Quan, Y. Hou, and H. Cheng, "Estimating pore volume compressibility by spheroidal pore modeling of digital rocks," *Petroleum Exploration and Development*, vol. 47, no. 3, pp. 603–612, 2020.